The effect of Ni impurities on some structural properties of pyrite thin films

1995 J. Phys.: Condens. Matter 7 2115

(http://iopscience.iop.org/0953-8984/7/10/018)

J. Phys.: Condens. Matter 7 (1995) 2115–2121. Printed in the UK

The effect of Ni impurities on some structural properties of pyrite thin films

I J Ferrer, C de la Heras and C Sánchez

Departamento Física de Materiales, C-IV and Instituto Nicolás Cabrera, Universidad Autónoma de Madrid, UAM, Cantoblanco, 28049 Madrid, Spain

Received 31 October 1994

Abstract. Thin films of $Fe_{1-x}Ni_xS_2$ ($0 \leqslant x \leqslant 1$) solid solutions have been prepared by sulphuration of Fe–Ni layers previously flash evaporated. Their structural properties have been investigated by x-ray diffraction (XRD) as a function of the sulphuration temperature and Ni/Fe atomic ratio. The dependence of the lattice parameter on the Ni/Fe atomic ratio shows that Ni increases the dimensions of the unit cell, which appears to be initially compressed.

1. Introduction

Iron disulphide pyrite (FeS_2) is considered as a good semiconductor useful for solar applications not only due to its adequate physical properties but also for the possibility of obtaining p- and n-type samples [1]. Our interest is focused in making an n-FeS_2/p-FeS_2 photovoltaic device. In this respect a systematic study of the effect of some impurities on different properties of the material is being carried out in our laboratory [2, 3]. The present paper reports on the correlation between the chemical composition and the structural properties of pyrite thin films doped with Ni. Ni was chosen to obtain n-type thin films since, up to now, the films prepared in our lab were p-type [4] or of undefined conductivity [5]. Moreover, Ni is one of the most abundant impurities in natural single crystals of pyrite [1, 6–8] and it is also a contaminant in synthetic single crystals [9, 10] due to its presence as impurity in the precursor. The effect of Ni in pyrite single crystals has been studied by electron paramagnetic resonance (EPR) [9–11] in samples in which it appears as a contaminant [9, 10] and in samples in which it was artificially incorporated [11], and it has been concluded that Ni resides in the Fe^{2+} lattice positions as Ni^{2+}. The correlation of the Ni presence with the optoelectronic properties of pyrite single crystals has been also investigated [7] although only preliminary conclusions have been reached.

The influence of the lack of stoichiometry on the pyrite microstructure and some implications on its electronic properties have been investigated [12, 13]. The non-stoichiometry has been related to S vacancies, which can affect the pyrite band structure and its lattice parameter. However, few results concerning the influence of impurities on the structural properties have been published. In this respect Tributsch *et al* have studied the structural properties of $Ru_xFe_{1-x}S-2$ solid solutions [14], reporting a continuous lattice parameter increase as x is increased.

0953-8984/95/102115+07$19.50

2. Experimental details

Three series of Fe–Ni layers have been prepared by flash evaporation on glass substrates. The initial source of every series contains a different proportion of Ni mixed with Fe powder: 0.5 at.%, 2 at.% and 10 at.%. For comparison Fe and Ni films were also evaporated. Every film was finally sulphurated under a sulphur atmosphere in a vacuum sealed glass ampoule for 20 h at temperatures, T_s, between 250 and 500 °C. The experimental procedure has been previously described [5].

The structure of the films was identified by x-ray diffraction (XRD) in a Siemens D5000 automated x-ray diffractometer with Cu Kα radiation. Stoichiometry and Ni concentration of the films were estimated by energy dispersive analyses of x-rays (EDAX). Film morphology was investigated by scanning electron microscopy (SEM). Film thicknesses were measured with a mechanical stylus Sloan Dektak IIA.

3. Results and discussion

The thickness of the initial metallic layers was about 0.3–0.4 μm. After annealing treatment the thickness increased to 0.8, 0.8, 1.0 and 1.5 μm for the series with Ni nominal content of 0, 0.5, 2 and 10 at.%, respectively. The Ni metallic layer was 0.2 μm thick and increased to 0.7 μm after sulphuration.

The Ni concentration, estimated by EDAX, was 4.5 at.% and 25 at.% for the 2 and 10 at.% nominal Ni concentration series, respectively. In both cases the Ni content seems to be higher than that in the initial source. This result is in agreement with the conclusion of Siebert *et al* [9] that the pyrite structure favours its enrichment in Ni during the crystallization. The amount of Ni in the lowest-content series is below the detection limit of EDAX. However, from the results of the Ni/Fe ratio for the other series it could be estimated as 1.1–1.2 at.%. The stoichiometric ratio, defined as S/(Fe+Ni), varies from 1.8 to 2.3 with an error of ± 0.1. Therefore, series will henceforth be denoted by their composition as $Fe_{1-x}Ni_xS_2$ where $x = 0$, 0.012, 0.045, 0.25 and 1.

The structure of the samples was identified by XRD. Spectra of $Fe_{1-x}Ni_xS_2$ ($0 \leqslant x \leqslant 1$) samples sulphurated at 350 °C are depicted in figure 1, where several significant facts can be observed. Starting from $x = 0$ (figure 1(a)) one can see the pattern corresponding to the pyrite (FeS_2) structure. However, as Ni content in the sample increases all the diffraction lines are shifted towards smaller diffraction angles and at $x = 0.25$ (figure 1(d)) two phases (pyrite and vaesite) appear. The continuous shift of the XRD peak positions implies that the mixed compounds ($Fe_{1-x}Ni_xS_2$, where $x = 0.012$ and 0.045) crystallize in an unique structure, pyrite. The cause of the peak shift will be discussed below. In the absence of Fe ($x = 1$, figure 1(e)) only vaesite (NiS_2) is observed. Note that in films with $x = 0.25$ vaesite peaks are shifted to higher diffraction angles (compare figure 1(e) with 1(d)) and pyrite ones to lower angles (compare figure 1(d) with 1(a)). It is worth emphasizing that pyrite (FeS_2) and vaesite (NiS_2) crystallize with the same cubic structure ($Pa\bar{3}$ space group), their lattice parameters being $a_0 = 5.417$ Å (ASTM 6-0710) and $a_0 = 5.670$ Å (ASTM 11-99), respectively.

The $Fe_{1-x}Ni_xS_2$ ($x = 0.25$) films also show an unique pyrite structure at $T_s < 350$ °C but at $T_s \geqslant 350$ °C two segregated phases can be observed, pyrite and vaesite. This result agrees with those of Chandler and Bené [11], who found that the growth of $Fe_{1-x}Ni_xS_2$ crystals with pyrite structure had a limited range of chemical composition ($x \leqslant 0.1$). Other authors [15, 16] have also found that the disulphides of Fe and Ni do not form extensive

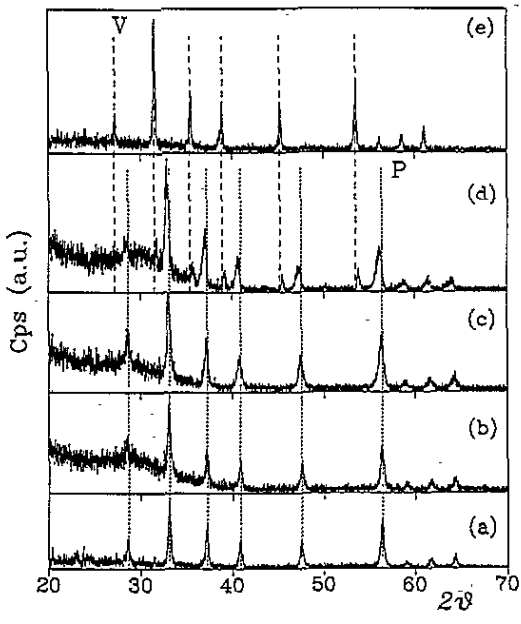

Figure 1. XRD spectra of $Fe_{1-x}Ni_xS_2$ samples sulphurated at 350 °C: (a) $x = 0$, (b) $x = 0.012$, (c) $x = 0.045$, (d) $x = 0.25$ and (e) $x = 1$. P and V mean pyrite (FeS_2) and vaesite (NiS_2) structure.

solid solutions between them as deduced by the phase diagram of the Fe–Ni–S system [16]. However, mixed disulphides $(Fe, Ni)S_2$ have been observed in some mineralized areas and have been considered as a metastable phase [17]. This phase, named bravoite, represents an intermediate phase between pyrite and vaesite with $a_0 = 5.510$ Å [17, 18]. The fact that pyrite structure appears at lower T_s than vaesite, in samples with similar Ni contents, could suggest that pyrite has a lower heat of formation than vaesite. In fact, values of heat of formation calculated by Rosenqvist [15] confirm this conclusion.

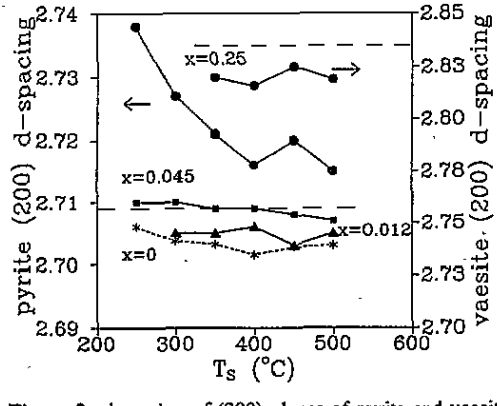

Figure 2. d spacing of (200) planes of pyrite and vaesite in $Fe_{1-x}Ni_xS_2$ films as a function of sulphuration temperature. The dotted lines correspond to the pyrite and vaesite ASTM values. (x values are given to identify each film series.)

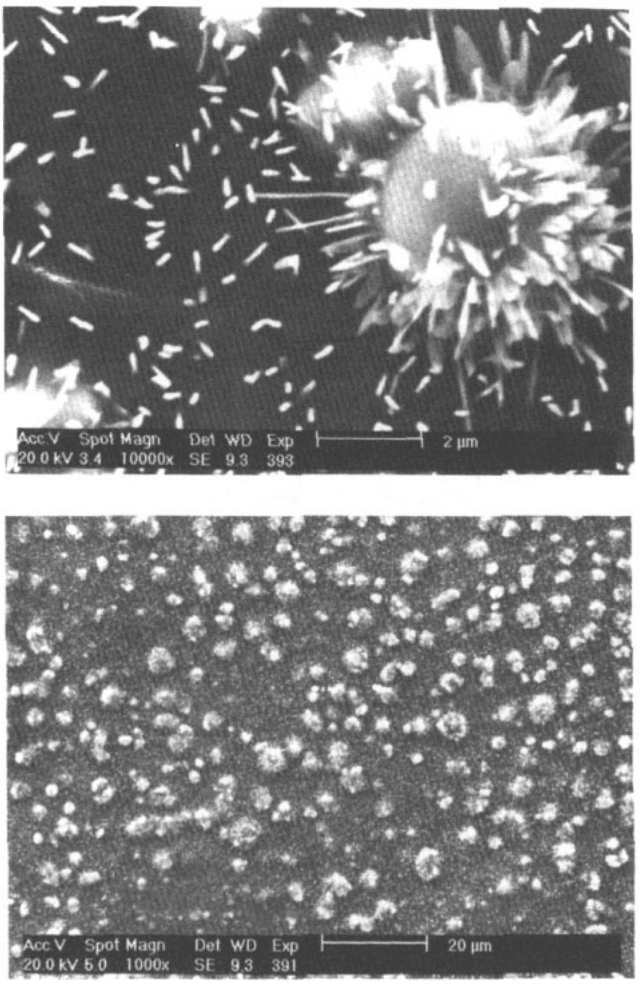

Figure 3. SEM micrographs of an $Fe_{1-x}Ni_xS_2$ ($x = 0.25$) film sulphurated at 400 °C, at two different magnifications.

Since pyrite crystallizes with cubic structure, the (200) d spacing is proportional to the lattice constant. Hence, we will use this parameter (calculated from the position of the (200) peak) to study the influence of sulphuration temperature and Ni content in the unit cell. Figure 2 shows the dependence of (200) d spacing on the sulphuration temperature for the different Ni content series. The first significant fact observed is that FeS_2 ($x = 0$) films show a lower (200) d spacing than that appearing in ASTM tables ($d = 2.709$ Å), which suggests that the film lattice dimension ($a_0 = 5.406$Å) is also smaller than that from ASTM ($a_0 = 5.417$ Å). This fact could be explained by assuming that undoped as-prepared films have a large density of iron and sulphur vacancies (V_{Fe} and V_S, respectively), which compress the lattice. Similar effects of lattice compression have been observed in different materials. For example, in metallic lattices such as Ni and Pd, the formation of vacancies has been evidenced by the contraction of the lattice [19, 20]. In binary compounds this contraction can be generated by both cationic and anionic vacancies. So, Semiletov [21]

established a linear dependence between the change in composition and the decrease of the lattice constant in GaAs, which was demonstrated to be due to the formation of Ga vacancies. Furthermore, Krill *et al* [22] used the lattice parameter as a measure of the Ni vacancy concentration in NiS_2. They showed that the lattice compression (observed in a given range of stoichiometry) was due to the Ni vacancy formation since the fraction of S vacancies in the S sublattice was kept constant. Tributsch *et al* [13] also found a similar linear relation between the change in composition and the lattice compression in FeS_2. However, they attributed the lattice contraction only to S vacancies.

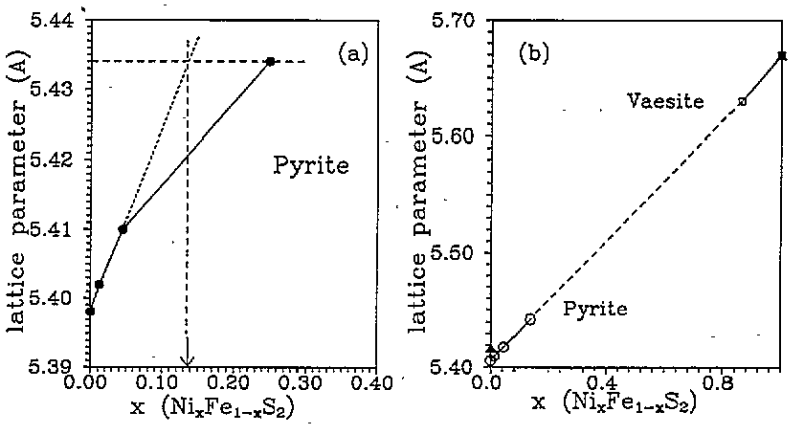

Figure 4. (a) Lattice parameter of pyrite against Ni content (x), (b) lattice parameter against Ni content estimated by EDAX and extrapolated from (a). ▲ corresponds to ASTM values for pyrite and vaesite lattice parameters.

From figure 2 it is also evident that the presence of Ni in the films leads to an increase of the lattice parameter, suggesting the expansion of the lattice. This fact is readily explained by assuming, as established by EPR [9, 10], that Ni resides as Ni^{2+} in the Fe^{2+} positions. In this way, Ni can be incorporated by two mechanisms that can produce lattice expansion: on one hand, if Ni occupies Fe vacancies it contributes to decreasing the Fe vacancy density, expanding the lattice; on the other hand, if Ni substitutes Fe atoms the (200) d spacing also increases (since the (200) d spacings of vaesite and pyrite are $d = 2.835$ Å and 2.709 Å, respectively). In both cases the magnitude of the lattice expansion should be dependent upon the amount of Ni as observed in the experimental results. Curiously, the $Fe_{1-x}Ni_xS_2$ ($x = 0.045$) series has a similar (200) d spacing as appears in the ASTM tables for pyrite.

At higher Ni amounts ($x = 0.25$ series) the pyrite (200) d spacing is still higher, as expected. However, it decreases as T_s is increased up to 350 °C, the T_s at which two phases appear (pyrite and vaesite). The higher values of (200) d spacing at $T_s < 350$ °C, compared with those at $T_s > 350$ °C, are attributed to the higher Ni content in the pyrite lattice since NiS_2 is not formed yet. At $T_s > 350$ °C the high value of the (200) d spacing of pyrite (figure 2) and the low value of the vaesite one (both compared with ASTM data) are due to the presence of Ni in pyrite and Fe in vaesite. At this point, it is worth emphasizing that the value of x, measured by EDAX, is an average of the Ni content in the whole surface and, therefore, the actual x value must be different in pyrite than in vaesite microcrystals. In fact, samples of the $x = 0.25$ series have rather inhomogeneous morphology as viewed by SEM. The higher the sulphuration temperature, the more inhomogeneous is the surface.

As an example, figure 3 shows the SEM morphology of a film sulphurated at 400 °C. As can be observed there are balls of about 3 μm size, in which the Ni content (estimated by EDAX) is about 30% higher than that in the background layer.

The pyrite lattice constant, calculated from the (200) d spacing, is plotted in figure 4(a) as a function of Ni content, x, in the films at a given sulphuration temperature ($T = 350$ °C). As can be observed the pyrite lattice constant increases as Ni content is increased. Since x is an average value and assuming that the pyrite (200) d spacing must be linear in x, one can estimate the real value of x in the pyrite polycrystals of the films with $x = 0.25$. So, by extrapolation of the a_0 values for films with $x < 0.25$ in which vaesite does not appear, to the value of a_0 for $x = 0.25$, as indicated in figure 4(a), we obtain that the Ni content (x) in pyrite microcrystals is 0.135. Therefore, assuming that the rest of the Ni is only in the form of vaesite, the Ni content (x) of vaesite polycrystals in the same films would be 0.865. Now, the pyrite and vaesite lattice parameter against the measured and estimated values of x are plotted in figure 4(b). As can be observed, the pyrite lattice constant increases in the presence of Ni and, in contrast, the vaesite lattice constant decreases in the presence of Fe, as expected from the above discussion. This effect has also been observed by Krill *et al* [22] by introducing Fe impurities into NiS_2 lattice in concentrations of up to 15 at.%.

The electrical properties, measured by the Hall effect, showed that the films with $x = 0.045$ have n-type conductivity with Hall mobilities from 5 to 20 $cm^2\ V^{-1}\ s^{-1}$ and carrier densities of 10^{18}–10^{20} cm^{-3}, depending on the sulphuration temperature [23]. However, Hall effect measurements with the other series ($x = 0$, 0.012 and 0.25) did not yield any conclusive result. In the films with $x = 0$ and 0.012, this behaviour can be attributed to V_{Fe}–V_S compensation since V_{Fe} act as acceptors and V_S as donors. This compensation effect disappears in the films with $x = 0.045$ due to the considerable reduction of V_{Fe} produced by Ni atoms and the films become n-type. In the films with $x = 0.25$ the reason could be the inhomogeneity of the samples.

4. Conclusions

The lattice parameter of the pyrite thin films in the absence of Ni at every sulphuration temperature used here (250 °C< T_S < 500 °C) is lower than the standard (ASTM) value, suggesting compression of the lattice, probably due to the presence of sulphur and iron vacancies.

The pyrite lattice parameter increases as Ni is introduced into the lattice. Two effects could lead to this expansion: reduction of the Fe vacancy density by inclusion of Ni and substitution of Fe by Ni. From electrical measurements, we conclude that Ni occupies Fe vacancies since the samples with $x = 0.045$ have n-type conductivity. The vaesite lattice parameter decreases due to the presence of Fe in Ni sites.

Acknowledgments

The authors thank Mr F Moreno and Mr F Caballero for technical assistance in the sample preparation. Support given by the Comisión Interministerial de Ciencia y Tecnología (CICYT) under contract No MAT 0199/91 and Comunidad Autónoma de Madrid (CAM) with reference C-C042/91 is also acknowledged.

References

[1] Shuey T 1975 *Semiconducting Ore Minerals* (Amsterdam: Elsevier) p 304 and references therein
[2] Ferrer I J, de las Heras C and Sánchez C 1993 *Appl. Surf. Sci.* **70/71** 588
[3] Ferrer I J, Caballero F, de las Heras C, Sánchez C 1994 *Solid State Commun.* **89** 349
[4] de las Heras C and Sánchez C 1991 *Thin Solid Films* **199** 259
[5] Ferrer I J and Sánchez C 1991 *J. Appl. Phys.* **70** 2641
[6] Ferrer I J and Sánchez C 1992 *Solid State Commun.* **81** 371
[7] Fiechter S, Hartmann A, Dulski P, Jokisch D and Tributsch H 1992 *Non-stoichiometry in semiconductors* ed K J Bachmann, H-L Hwang and C Schwab (Amsterdam: Elsevier) p 87
[8] Schieck R, Hartmann A, Fiechter S, Könenkamp R, Wetzel H 1990 *J. Mater. Res.* **5** 1567
[9] Siebert D, Miller R, Fiechter S, Dulski P and Hartmann A 1990 *Z. Naturf.* a **45** 1267
[10] Yu J-T, Wu C, Huang Y and Lin S 1992 *J. Appl. Phys.* **71** 370
[11] Chandler R N and Bené R W 1973 *Phys. Rev.* B **8** 4979
[12] Birkholz M, Fiechter S, Hartmann A and Tributsch H 1991 *Phys. Rev.* B **43** 11 926
[13] Fiechter S, Birkholtz M, Hartmann A, Dulski P, Giersig M, Tributsch H and Tilley R J 1992 *J. Mater. Res.* **7** 1829
[14] Lichtenberger D, Ellmer K, Schieck R, Fiechter S and Tributsch H 1994 *12th Eur. Photovoltaic Solar Energy Conf. (Amsterdam, 1994)*
[15] Rosenqvist T 1954 *J. Iron Steel Inst.* **176** 37
[16] Craig J R and Scott S D 1976 *Sulfide Mineralogy (Reviews in Mineralogy)* vol I, ed P H Ribbe (Washington, DC: Mineral Society of America)
[17] Springer G, Schachner-Korn D and Long J V P 1964 *Econ. Geol.* **59** 475
[18] Shimazaki H 1971 *Econ. Geol.* **66** 1080
[19] Fukai Y and Okuma N 1993 *Japan. J. Appl. Phys.* **32** L1256
[20] Semiletov S A, Barranova R V, Khodyrev Y P and Imamov R M 1980 *Sov. Phys.–Crystallogr.* **25** 665
[21] Semiletov S A 1967 *Sov. Phys.–Crystallogr.* **12** 277
[22] Krill G, Lapierre M F, Gautier F, Robert C, Czjzek G, Fink J and Schmidt H 1976 *J. Phys. C: Solid State Phys.* **C9** 761
[23] Ferrer I J, de las Heras C and Sánchez C 1994 *Transport Properties of Ni-doped FeS_2 Films* to be published